



JOURNAL OF
SYNCHROTRON
RADIATION

Volume 28 (2021)

Supporting information for article:

**Redox State and Photoreduction Control using X-ray
Spectroelectrochemical Techniques – Advances in Design and
Fabrication Through Additive Engineering**

**Stephen Peter Best, Victor A. Streltsov, Christopher Thomas Chantler,
Wangzhe Li, Philip A. Ash, Shusaku Hayama and Sofia Diaz-Moreno**

S1. Outline of the layout and elements of the stepper motor drive assembly

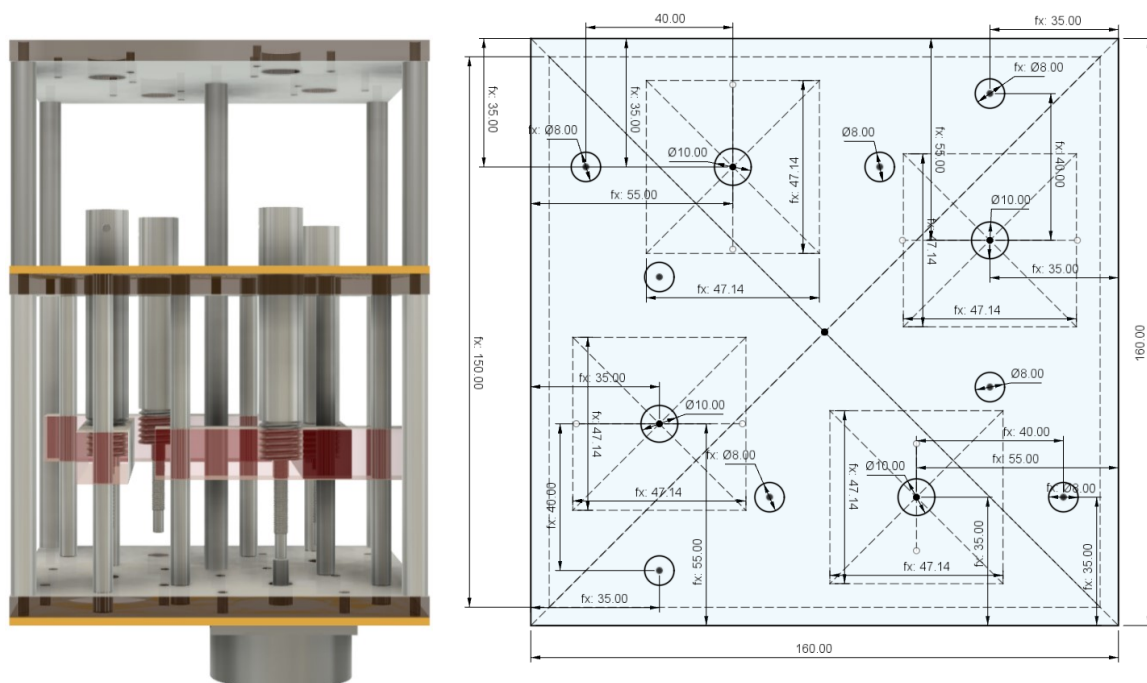


Figure S1 3D CAD representations of the 4-position stepper motor assembly (Left) and technical drawing of the layout of the bottom layer of the assembly (Right).

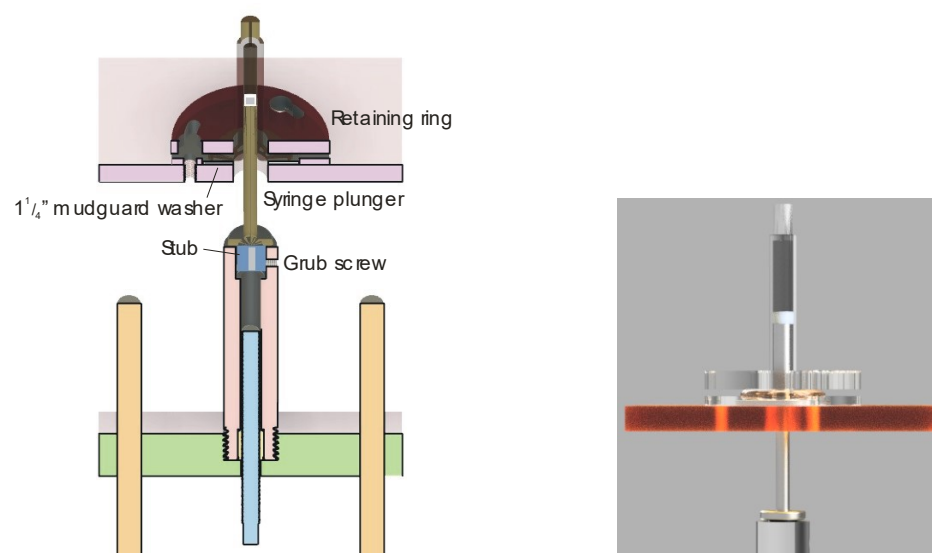


Figure S2 Details of the attachment of the gas-tight syringe to the stepper motor drive assembly. Cross-section view (left) and CAD rendered view (Right). The flanged part of the syringe barrel is tethered to the top layer of the assembly by clamping between a washer and retaining ring.

S2. Stepper Motor Controller Program

The KTA290 stepper motor controller is operated through a USB port and supports the simultaneous control of up to 4 axes. The control program needs to satisfy at least 3 functions. (1) Establish software limits based on the syringe capacity and fill state. (2) Facilitate a linear flow with a controlled flow rate and volume, including contained flow between syringes in a closed system. (3) Support pulsed flow in a closed system with control over the outward and return flow volumes, cessation of flow or reversal of the net flow direction in reaching a specified net flow volume.

The implementation of these functions is illustrated with reference to the forms comprising the relevant functions in the application.

The main window (Figure S3) provides information on the status of the stepper motors and a summary of the hardware and certain commands sent to and from the controller.

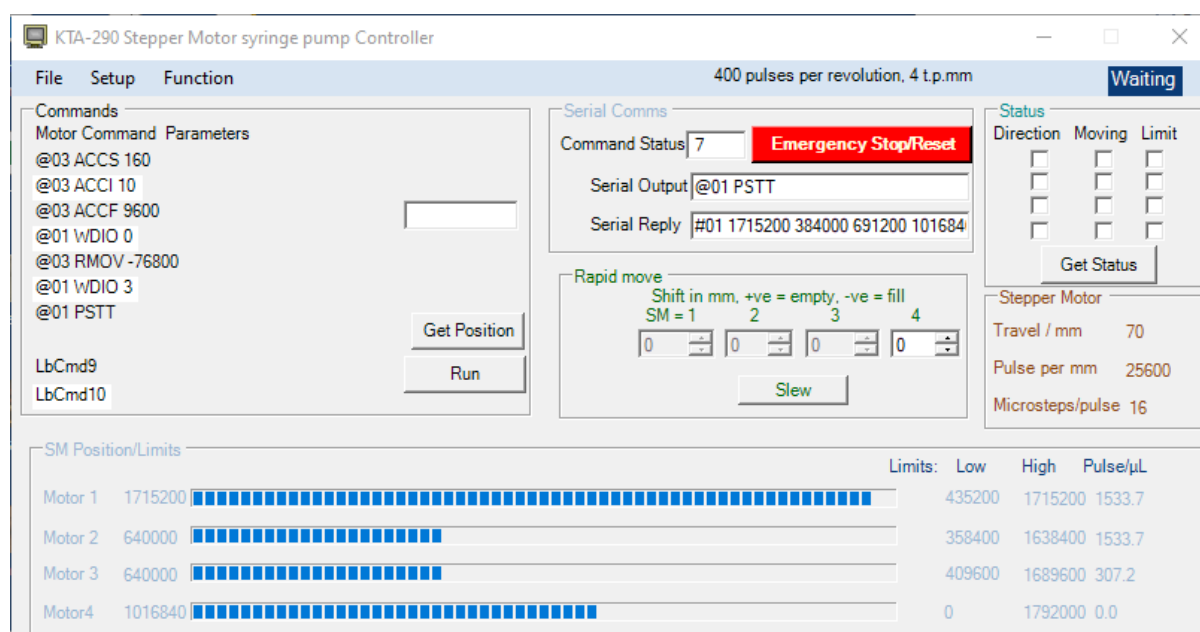


Figure S3 The main menu

The physical limits of translation of the syringe plunger are set in the SetSyringe form (Figure S4). The syringe size, initial solution volume, maximum solution volume and projection of the plunger beyond the body of the syringe need to be associated with the syringe positions. Further, since slewing of the motors are inactivated when a syringe is set, a flag identifies whether a syringe is set at the syringe positions. Once set the low and high limits of movement and the number of pulses per μ L are updated in the main menu.

Figure S4 The form used to input the properties of the syringes attached to the syringe driver.

The flow form (Figure S5) facilitates translation of the plunger of one or more syringes at a specified velocity in terms of the number of stepper motor pulses per second. If a syringe has been set for the selected motor then the number of seconds needed to flow 1 μL is reported. Simultaneous flow of the syringes is maintained either until a specified translation of the plunger or a volume of solution (if a syringe has been set) is complete. The program will adjust the end point so as to be consistent with the low and high limits of movement given in the main menu. The stepper motor controller supports different flow rates and end times for the individual axes and it is straightforward to flow in the solution between syringes in a closed system.

Motor	Pulse/s	secs/ μL	Volume/ μL or mm	Time/s
1	100	15.34	50	766.8635
2	10	153.37	0	0
3	10	30.72	0	0
4	10	not set	0	0.00

+ve = empty, -ve = fill

@01 ACCF 100 10 10 10
@01 RMOV 76686 0 0 0

Figure S5 The form used to control linear flow of the solutions.

The pulsed flow menu (Figure S6) allows flow between matched syringes. When a syringe is set the source and receiver radar items are activated and the number of stepper motor pulses per μL is reported, allowing identification of matched syringes. The pulse width corresponds to the forward flow volume (in nL) and the net flow is adjustable between 0 and the pulse width. The pulsed flow will continue in the set direction until the limit is reached with either syringe. If the reverse flow on the limit box is checked then the pulsed flow will continue, but with the definitions of the source and receiver syringes reversed. If the Use current as limit box is checked then the reversed flow will continue until the current syringe position is reached. The limit flow check box will allow the setting of the flow limits to a specified volume (e.g. 100 μL). In this case the current position is set as one limit and the other is set according to the net volume flow.

Syringe (SMpulses/ μL)		Source	Receiver	SM limits	
				min	max
1	1533.7	<input type="radio"/> RB1s	<input checked="" type="radio"/> RB1r	1561827	1715200
2	1533.7	<input checked="" type="radio"/> RB2s	<input type="radio"/> RB2r	640000	793373
3	307.2	<input type="radio"/> RB3s	<input type="radio"/> RB3r	409600	1689600
4	not set	<input type="radio"/> RB4s	<input type="radio"/> RB4r	0	1792000

Pulse width/nL: 500 ☒ Reverse flow on limit

Net flow (nL)/cycle: 50 ☒ Limit flow volume: 100 μL

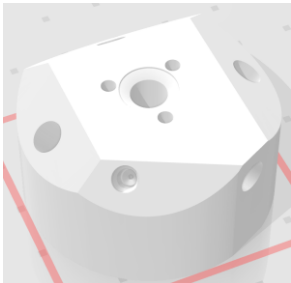


out	2	@01 RMOV -767 767
in	1	@01 RMOV 690 -690
out	1	@01 RMOV 767 -767
in	2	@01 RMOV -690 690

Update syringe props

Start Pulsed Flow

Figure S6 The form used to setup the pulsed flow mode of operation.

S3. 3D Files (STL format generated using OpenSCAD) suitable for 3D printing the XAS-SEC cell.**Table S1** Details of the STL files available for download

Component	Filename	Filesize	Image
Cell body	RT-XAS-SECell_body.stl	6.15 MB	
Counter electrode holder	RT-XAS-SECell_counter.stl	1.45 MB	
Front window	RT-XAS-SECell_front.stl	3.75 MB	

Note that straight holes are printed of a diameter suitable for tapping.

S4. Variation of the open circuit potential (OCP) during XAS measurements at the I20-scanning beamline of the DLS

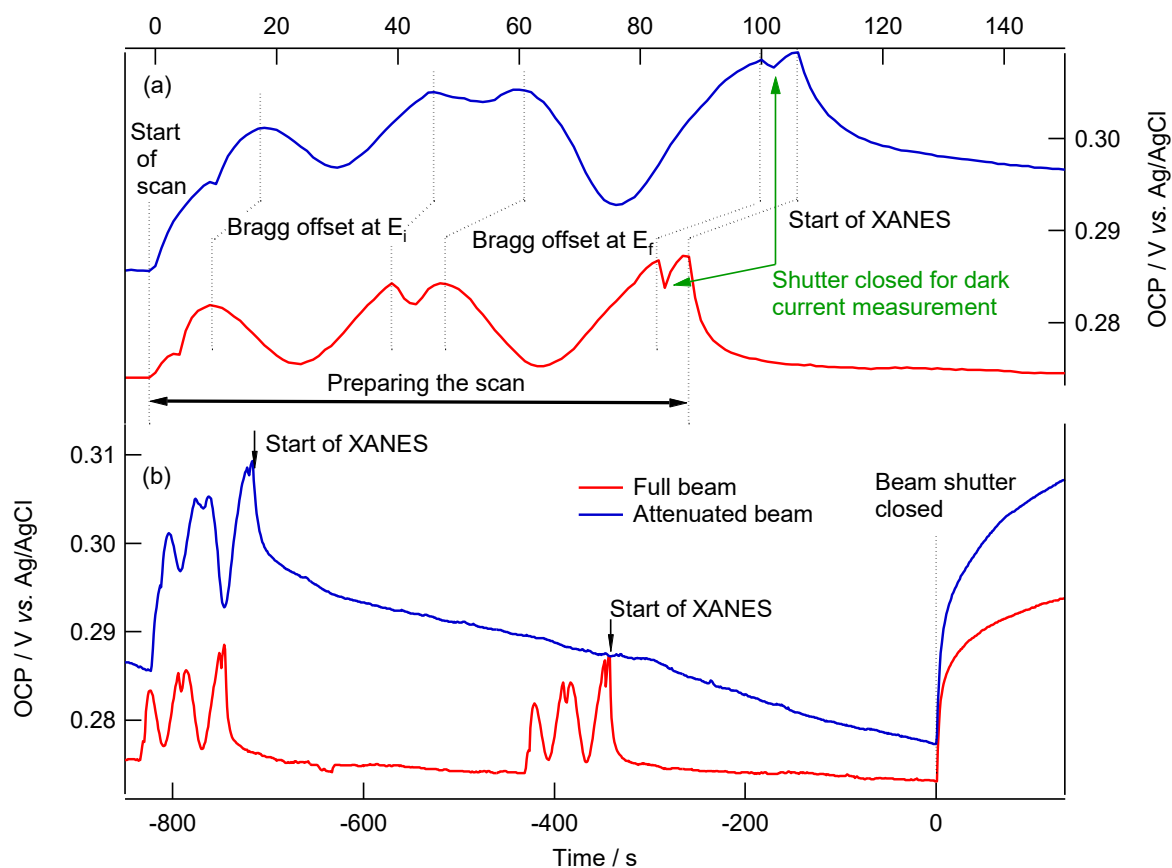


Figure S7 Variation of the open circuit potential (OCP) with time during measurement of the XANES of $[\text{CuCl}(\text{bpy})_2]^+$. (a) expanded view during the monochromator alignment protocol and dark current measurements. During this procedure the shutter is open and the monochromator moved to the start of the scan, then the second downstream axis is scanned with respect to the upstream axis to identify the optimal alignment setting. This procedure is repeated at the end of the scan energy. During this alignment process the transmission of X-rays through the monochromator is changing and only at the maximum when the two Bragg axes are in alignment. This is reflected by the dip in the OCP. The different scan range for the full beam and attenuated beam experiments is responsible for difference in alignment time. (b) The OCP response for the full and attenuated beam scans as shown in Figure 5. In this plot the full set of data for the attenuated beam scan (XANES and EXAFS regions) is given. Approximately two XANES scans (full beam) were recorded over this timescale.

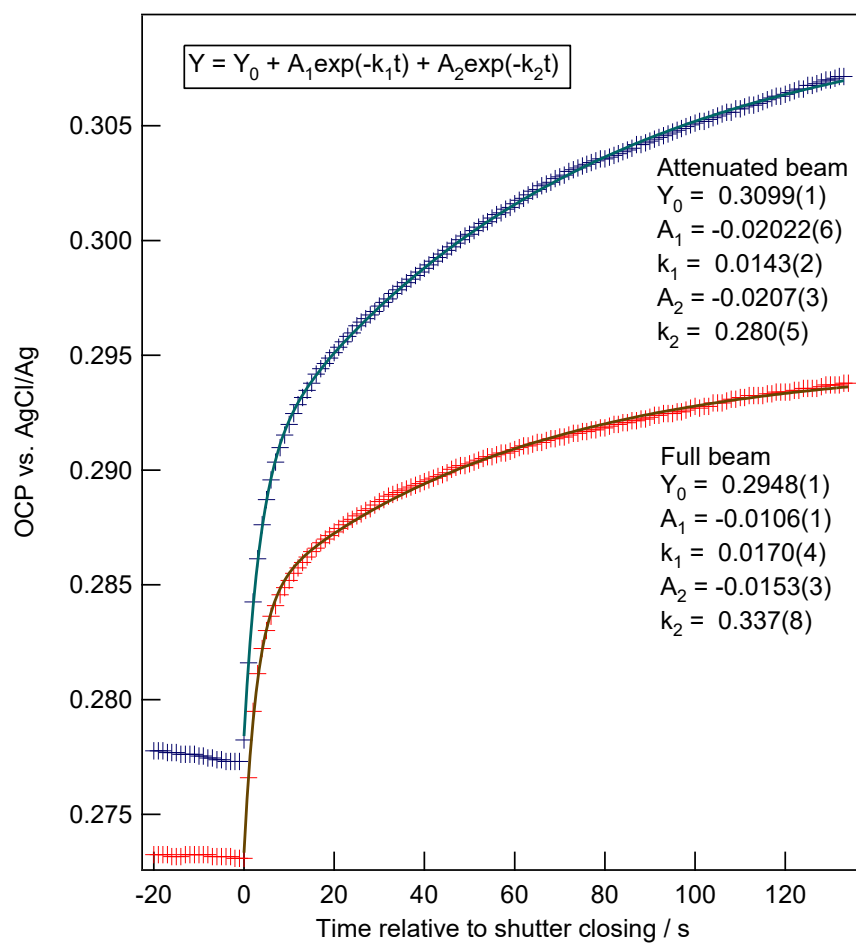


Figure S8 Fit of the changes in OCP in response to closing the shutter at the end of the scan. The decay is fitted to a double exponential using IgorPro software (Wavemetrics). The fitting function, refined parameters and estimated standard deviations are included in the figure.